FLOW FIELD INVESTIGATION OF A GROUNDED HELICOPTER FUSELAGE IN CROSSWIND CONDITIONS

Alberto Fabbris, Research Engineer, a.fabbris@hit09.com, HIT09 Srl (ITALY), www.hit09.com

Rita Ponza, Senior Research Engineer, r.ponza@hit09.com, HIT09 Srl (ITALY), www.hit09.com

Ernesto Benini, Associate Professor, ernesto.benini@unipd.it, University of Padova (ITALY)

Abstract

The aerodynamic characteristics of a grounded medium class helicopter fuselage operating in crosswind conditions have been calculated by means of Computational Fluid Dynamics (CFD) in order to propose an experimental strategy for a Wind Tunnel (WT) testing program. The aim of this work is to determine Drag Force F_D and Yaw Moment M_x on the fuselage for helicopter rollover prevention following a correct characterization in CFD and subsequently in WT of the Atmospheric Boundary Layer (ABL). In order to provide confidence on CFD outputs, an isolated fuselage configuration was first analyzed and the associated simulation results compared against the available WT data. Then the grounded fuselage was analyzed providing the ground effect on the fuselage aerodynamic characteristics. The drag force acting on the fuselage is doubled when the aircraft is nearby the ground, consequently both the pitch and yaw moments are increased with respect to the values encountered when considering a free stream flow over the fuselage.

The reduced model scale for the experiments will lead to an increase of the experiment complexity, caused by the scaled reduction of the vertically logarithmic distribution of mean wind speed and turbulence quantities due to the related decrease in z_0 value.

Notation

Symbols

ABL	Atmospheric Boundary Layer
C_S	Roughness Constant
E	Empirical Constant
F_D	Drag Force
K_S	Roughness Height
M_x	Yaw Moment
M_z	Pitch Moment
WT	Wind Tunnel
*u**	Friction Velocity
u^*_{ABL}	*ABL friction velocity*,
z_0	Aerodynamic Roughness Length
z	Vertical Coordinate
ρ	Density
κ	von Karman constant
τ_w	Wall Shear Stress
$u_{\tau 0}$	Laminar Bottom Layer Friction Velocity
$C_\mu, \sigma_\kappa, \sigma_\varepsilon, C_{\varepsilon 1}, C_{\varepsilon 2}$	*k-ε* model constants

1. INTRODUCTION

In CFD simulation, the inlet boundary conditions of mean wind speed and turbulence quantities should represent the upcoming fully developed wind flow, a vertically logarithmic distribution of mean wind speed characteristic with friction velocity u* and aerodynamic surface roughness length z_0. If the wind is coming from a uniform flat terrain, the velocity and turbulence quantities distribution should not change along the same flat terrain in a suitable CFD velocity and turbulence model. This requirement is referred as horizontally homogeneous ABL flow over uniformly rough terrain. Many authors [1,2] reported the difficulties encountered to get horizontal homogeneity, concluding that the horizontal variance partially comes from the disagreement between standard wall functions with a sand-grain-based roughness height modification in some commercial CFD codes and ABL profiles characterized with aerodynamic roughness length. Furthermore the simulation of helicopter fuselage needs an unstructured grid with an average surface y+ of 30 which the sand-grain-based models can't allow. A remedial method [3,4] is provided in this paper considering to directly set constant wall shear stress to the ground boundary of the domain and it could be adopted as a substitute of unacceptably large roughness height allowing the use of a more refined grid. The wind profile of horizontal velocity and the dissipation rate of kinetic

energy for the ABL flows were directly proportional to the ABL friction velocity, basing on the assumption that the turbulence kinetic energy (TKE), as well as the shear stress, is constant along the z coordinate. If the flow field is described in this way, wall shear stress should be directly deduced as a function of the distance from the center point of wall adjacent cell to wall surface, the velocity in the center of the same point, the density of the air, the constant TKE and the aerodynamic surface roughness length z_0. Definition of shear stress requires, therefore, a refinement of the ground adjacent cells through definition of the Boundary Layer, where the total height must be equal to the z_0.

2. FUNDAMENTAL MATHEMATICAL MODELS

2.1. RANS equations and k-ε two-equation turbulence model

Reynolds-Averaged Navier Stokes equations are written in Cartesian coordinates:

(1) $$\frac{\partial \rho}{\partial t} + \frac{\partial}{\partial x_i}(\rho u_i) = 0$$

(2) $$\frac{\partial}{\partial t}(\rho u_i) + \frac{\partial}{\partial x_i}(\rho u_i u_j) = -\frac{\partial p}{\partial x_i} + \frac{\partial}{\partial x_j}\left[\mu\left(\frac{\partial u_i}{\partial x_j} + \frac{\partial u_j}{\partial x_i} - \frac{2}{3}\delta_{ij}\frac{\partial u_i}{\partial x_i}\right)\right] + \frac{\partial}{\partial x_j}(-\rho\overline{u_i u_j})$$

Where (1) is continuity equation, (2) are momentum equations, u is ensemble-average velocity, - $\rho\overline{u_i' u_j'}$ are Reynolds stress which must be modeled. The standard *k-ε* model assumed that the flow is fully developed turbulence: for ABL that is fully aerodynamically rough, the shear stresses are dominated by Reynolds stress, and the effects of molecular viscosity are negligible. In incompressible air flow, Reynolds stress is modeled as [5]

(3) $$\overline{u_i' u_j'} = \mu_t\left(\frac{\partial u_i}{\partial x_j} + \frac{\partial u_j}{\partial x_i}\right) - \rho$$

In the *k-ε* model, two additional transport equations are solved to calculate the turbulent viscosity μ_t, one for the turbulence kinetic energy (TDE) *k* and the other one for the turbulent dissipation rate (TDR) *ε*, in neutral stratification, incompressible air flow without buoyancy effects, they are written as follows:

(4) $$\frac{\partial}{\partial t}(\rho k) + \frac{\partial}{\partial x_i}(\rho k u_i) = \frac{\partial}{\partial x_j}\left[(\mu + \frac{\mu_t}{\sigma_k})\frac{\partial k}{\partial x_j}\right] + P_k - \rho\varepsilon$$

(5) $$\frac{\partial}{\partial t}(\rho\varepsilon) + \frac{\partial}{\partial x_i}(\rho\varepsilon u_i) = \frac{\partial}{\partial x_j}\left[(\mu + \frac{\mu_t}{\sigma_\varepsilon})\frac{\partial \varepsilon}{\partial x_j}\right] + C_{1\varepsilon}\frac{\varepsilon}{k}P_k - C_{2\varepsilon}\rho\frac{\varepsilon^2}{k}$$

Where σ_k , $C_{1\varepsilon}$ and $C_{2\varepsilon}$ are model constants, P_k represents the production of turbulence kinetic energy (evaluated in *k-ε* model with $P_k = \mu_t S^2$) where $S = \sqrt{2S_{ij}S_{ij}}$ is the modulus of the mean rate-of-strain tensor $S_{ij} = \frac{1}{2}\left(\frac{\partial u_i}{\partial x_j} + \frac{\partial u_j}{\partial x_i}\right)$. In standard *k-ε* model, turbulent viscosity is calculated by *k* and *ε* as

(6) $$\mu_t = \rho C_\mu \frac{k^2}{\varepsilon}$$

Where C_μ is a model constant with a commonly accepted value of 0.09 in industrial CFD simulation and 0.033 for ABL flow [4]. In a flat terrain ABL flow, a smaller C_μ means that, with stated turbulence intensity, the momentum transport is weaker, the gradient of mean velocity along height is larger. The *k-ε* model is a half empirical turbulence model so C_μ should be adjusted according to measurements.

Consider a flat terrain ABL flow which is steady, incompressible (*ρ=cost* , $\frac{\partial u_i}{\partial x_i} = 0$), 2D (*v= 0, w =0,* $\frac{\partial u}{\partial y} = 0$), high Reynolds number (μ « μ_t), with no buoyancy and streamwise homogenous ($\frac{\partial u}{\partial x} = 0, \frac{\partial k}{\partial x} = 0, \frac{\partial \varepsilon}{\partial x} = 0$). Then the transport equations of kinetic energy and dissipation rate of kinetic energy become:

(7) $$0 = \frac{\partial}{\partial z}\left[\frac{\mu_t}{\sigma_k}\frac{\partial k}{\partial z}\right] + P_k - \rho\varepsilon$$

(8) $$0 = \frac{\partial}{\partial z}\left[\frac{\mu_t}{\sigma_k}\frac{\partial \varepsilon}{\partial z}\right] + C_{1\varepsilon}\frac{\varepsilon}{k}P_k - C_{2\varepsilon}\rho\frac{\varepsilon^2}{k}$$

(9) $$P_k = \mu_t S^2 = \mu_t(\frac{\partial u}{\partial y})^2$$

The RANS equations could be simplified as

(10) $$\frac{\partial}{\partial x_i}(u_i) = 0$$

(11) $$\frac{\partial p}{\partial x} = \frac{\partial}{\partial z}\left((\mu + \mu_t)(\frac{\partial u}{\partial z})\right) \approx \frac{\partial}{\partial z}\left(\mu_t(\frac{\partial u}{\partial z})\right)$$

(12) $$\frac{\partial p}{\partial y} = \frac{\partial p}{\partial z} = 0$$

For the equations of momentum balance in *y* and *z* direction, the simplification process is similar.

2.2. ABL profile description

The Atmospheric Boundary Layer (ABL) is the lower part of the Earth's atmosphere and its behavior is directly influenced by the contact with the Earth's surface. Generally, the ABL could be divided into three parts vertically [6] as illustrated in Figure 1.

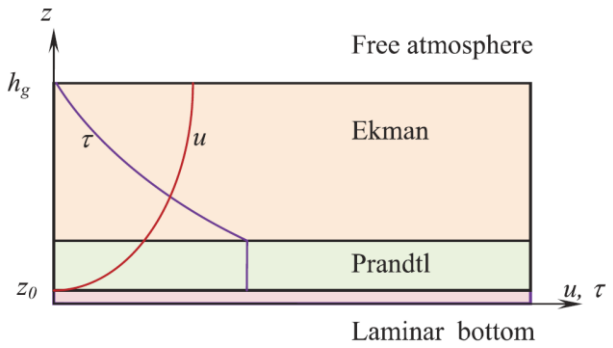

Figure 1: Subdivision of the AB with conceptual illustration of vertical distribution of horizontal velocity and shear stress within the boundary layer.

The lowest part is known as *laminar bottom layer* with a thickness equal to *aerodynamic roughness length* z_0, which is quite small compared to ABL height and could be neglected in most cases, so that $z \approx z + z_0$. For wind power engineering, typical values of roughness length [7] are shown in Table 1.

terrains	z_0 [m]
Muddy terrains, wetlands, icepack	$10^{-5} \div 3\ 10^{-5}$
Water areas *	$3\ 10^{-5} \div 0{,}0002$
Sand	$0{,}0002 \div 0{,}001$
Airport runway areas, mown grass	$0{,}001 \div 0{,}01$
Farmland/Airports with very few trees, buildings, *etc.*	$0{,}01 \div 0{,}04$
Many trees and/or bushes	$0{,}04 \div 0{,}1$
Forests, suburbs	$0{,}1 \div 1$
Cities	$1 \div 4$

Table 1: Typical surface roughness lengths

For this study, the airport runway was chosen to represent the ground and therefore z_0 is set equal to 0.005 [m].

3. WIND PROFILE WITH CONSTANT SHEAR STRESS

The following wind horizontal velocity profile, turbulent kinetic energy and kinetic energy dissipation rate are widely adopted for atmospheric boundary layer flows:

(13) $$u(z) = \frac{u^*_{ABL}}{\kappa}\ln\left(\frac{z+z_0}{z_0}\right)$$

(14) $$k(z) = \frac{{u^*_{ABL}}^2}{\sqrt{C_\mu}}$$

(15) $$\varepsilon(z) = \frac{{u^*_{ABL}}^3}{\kappa(z+z_0)}$$

where z is the vertical coordinate, u^*_{ABL} is the *ABL friction velocity*, here assumed equal to the *laminar bottom layer friction velocity* $u_{\tau 0}$

(16) $$u_{\tau 0} = \sqrt{\frac{\tau_w}{\rho}} = \sqrt{\frac{\mu}{\rho}\left.\frac{\partial u}{\partial z}\right|_{z=0}} = \sqrt{\upsilon\left.\frac{\partial u}{\partial z}\right|_{z=0}}$$

where τ_w is the ground shear stress; ρ is the density of air; μ and *v* are dynamic and kinematic viscosities, respectively; κ is the von Karman constant (≈0.40÷0.42).

For CFD simulation of turbulent wind flow based on RANS equation, the final flow field mostly depends on turbulence models and boundary conditions, especially ground wall treatment and other rational boundary settings. The ground surface is impossible to be described directly with fine meshes in CFD simulation, their effect to wind flow must be represented with near wall treatment functions.

Law-of-the-Wall [8] for mean velocity modified for roughness has the form

(17) $$\frac{u_p u^*}{\tau_w/\rho} = \frac{1}{\kappa}\ln\left(\frac{E z_p u^*}{\upsilon}\right) - \Delta B$$

Where suffix P means the center of wall adjacent cell, $u^* = C_\mu^{\frac{1}{4}} k^{\frac{1}{2}}$ is ABL friction velocity, k_p is TKE, $\tau_w = \rho u_{\tau 0}^2$ is shear stress, $u_{\tau 0}$ is ground surface friction velocity, which is assumed equal to u^*, *E* is an empirical constant whose value is set to 9.793, v is the kinetic viscosity.

ΔB depends on the type and size of the roughness and has been found to be well-correlated with the non-dimensional roughness height $K_s^+ = \frac{K_s u^*}{\upsilon}$.

For fully rough turbulent flow, namely $K_s^+ > 90$, that is the condition of ABL flow, ΔB is

(18) $$\Delta B = \frac{1}{\kappa}\ln(1 + C_s K_s^+)$$

Where C_S the is *roughness constant*; for fully rough turbulent flow with $C_S \in (0.5 ; 1)$, $C_s K_s^+ \gg 1$, then

(19) $$\Delta B \approx \frac{1}{\kappa}\ln\left(\frac{C_s K_s u^*}{\upsilon}\right)$$

With the assumption of $u_{\tau 0} = u^*$, combining equation (17) and (18), yields

(20) $$\frac{u_p}{u^*} = \frac{1}{\kappa}\ln\left(\frac{Ez_p}{C_s K_s}\right)$$

The wind velocity profile is described with $\frac{u_p}{u^*} = \frac{1}{\kappa}\ln\left(\frac{z_p}{z_0}\right)$, equation (20) must be equivalent with wind velocity profile, that is

(21) $$K_s = \frac{Ez_0}{C_s}$$

Equation (21) indicates the difference and relationship between *sand-grain-roughness height* and *wind flow aerodynamic roughness length*. For the default value of C_S = 0.5 and for the chosen roughness length z_0, the corresponding roughness height K_s will be about 10 [mm]; with the restriction that the center of wall adjacent cell should be higher than roughness height [8], the wall adjacent cell should be higher than 19.5 [mm], this is quite a coarse mesh and always unacceptable. However, this configuration was simulated as well in order to provide a reference point.

As indicated by [5,9], the problem of streamwise gradients over flat terrain encountered by some previous simulations with commercial CFD software is firstly caused by setting *roughness height* K_s as *aerodynamic roughness length* z_0.

From equation (26) we can get the wall shear stress in standard wall functions

(22) $$\tau_w = \frac{\rho\kappa C_\mu^{\frac{1}{4}} k^{\frac{1}{2}} u_p}{\ln\left(\frac{Ez_p}{C_s K_s}\right)}$$

Richard and Hoxey [5] indicated that the set of equations (10-12) is in accord with the transport equation of turbulence kinetic energy (8) and satisfies equation (9) under the following condition

(23) $$\kappa^2 = (C_{\varepsilon 2} - C_{\varepsilon 1})\sigma_\varepsilon \sqrt{C_\mu}$$

In order to simulate realistic atmospheric values of the TKE in the surface layer, it is necessary to use the constant set proposed in [4] properly modified to satisfy equation (23). The original and modified constants are visible in Table 2.

constants	C_μ	σ_κ	σ_ε	$C_{\varepsilon 1}$	$C_{\varepsilon 2}$
default	0.09	1.0	1.3	1.44	1.92
modified	0.033	1.0	2.38	1.46	1.83

***Table 2*: Default and modified model constants**

If the flow field is described as with equations (13,15), the wall shear stress should be deduced as:

(24) $$\left.\frac{\partial u}{\partial z}\right|_{z=z_p} = \frac{u^*}{\kappa z_p} = \frac{u_p}{z_p \ln(\frac{z_p}{z_0})}$$

(25) $$\mu_t = \rho C_\mu \frac{k^2}{\varepsilon} = \rho\kappa u^* z_p = \rho\kappa C_\mu^{\frac{1}{4}} k^{\frac{1}{2}} z_p$$

(26) $$\tau_w = \mu_t \left.\frac{\partial u}{\partial z}\right|_{z=z_p} = \frac{\rho\kappa C_\mu^{\frac{1}{4}} k^{\frac{1}{2}} u_p}{\ln(\frac{z_p}{z_0})}$$

Where subscript *p* denotes center point of wall adjacent cell and z_p is the distance from *p* to wall surface. Note that equations (13-15) are based on the assumption that the turbulence kinetic energy, as well as the shear stress is constant along height, that is

(27) $$\tau(z) = \mu_e \frac{\partial u}{\partial z} = \mu_t \frac{\partial u}{\partial z} = \rho C_\mu \frac{k^2}{\varepsilon}\frac{u^*}{\kappa z_p} = \rho u^{*2} = \tau_w$$

Where $\mu_e = \mu + \mu_t \approx \mu_t$ because $\mu_t \gg \mu$ in fully developed high Reynolds number turbulent flow.

Richard and Hoxey's method [5] adopted *roughness length* and logarithmic profile directly; in their method the wall shear stress is described as equation (26). These are equivalent if *roughness height* K_s is set according to equation (21) in Fluent. As indicated before, this would limit wall adjacent cell's fineness. In [5], Blocken *et al.* considered another choice that directly set wall shear stress with constant $\tau_w = \rho u^{*2}$ as a boundary condition, that will force $u_{\tau 0} = u^*$. This method could be adopted as a substitute of unacceptable large roughness height, but it only works for flat terrain with uniform roughness (wall shear stress will change over complex terrain).

Appropriate definition of Shear Stress requires, therefore, a refinement of the ground adjacent cells through the definition of the Boundary Layer, where the total height must be equal to the *Roughness Length* z_0. This method ensures to get *horizontal homogeneity* throughout the domain combined with an average surface y^+ of 30.

4. THE WIND ON A GROUNDED HELICOPTER: 3D ANALYSIS

CATIA®, GAMBIT®, TGRID® and ANSYS FLUENT® were used to accomplish the target of this work; specifically, CATIA® was needed to import the helicopter fuselage geometry, make it mesh-ready and generate the surface mesh; GAMBIT® and TGRID® were used both to create the virtual wind tunnel volume and create the volumetric mesh on

the fluid domain; ANSYS FLUENT® was chosen as the fluid dynamic solver.

GAMBIT® was used to create the far-field structured volumetric meshes so that the longitudinal (y axis) homogeneity throughout the domain was ensured; TGRID® was used to create the structured elements over the fuselage surface (the distance between the fuselage and the ground was set equal to 760 [mm]) in order to better simulate the physical boundary layer and to create the unstructured elements in the remaining of the fluid domain. The final volume mesh counts about 10.6 million mixed elements.

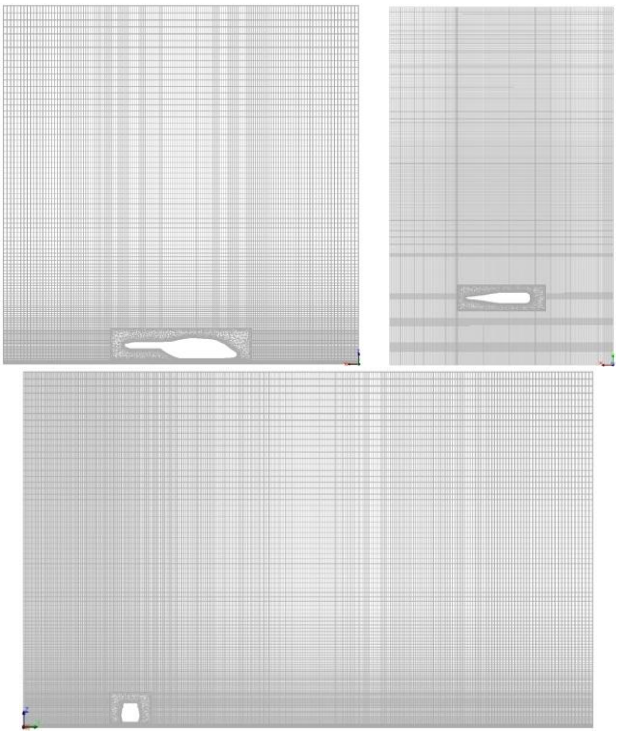

Figure 2: View of longitudinal and transversal sections of the whole domain volume mesh.

A wall shear condition was applied to the ground surface with shear stress in flow direction equal to τ_w=0.8081 [Pa]. For FLUENT® a series of User-Defined Functions (UDFs) were used to produce the profiles given by equations (13,14 and 15).

The following boundary conditions were prescribed: a velocity inlet condition was imposed on the WT inlet, while static pressure was assigned on the outlet section; a velocity inlet condition for the top of the domain with velocity value and turbulence values defined by z=50[m] (top of the boundary height). The fuselage surface was treated as a hydraulically smooth and adiabatic wall, while a symmetry condition was used for the lateral surfaces of the WT box. A pressure based solver with pressure-velocity coupling scheme was adopted as the solution algorithm. A second order discretization scheme for flow variables was used.

For each simulation, the convergence criterion was established when the RMS residuals were less than 1e-04 and the lift (z axis), drag (y axis), yaw moment (@ x axis) and pitching moment (@ z axis) reached an asymptotic trend. Furthermore, the difference between the mass flow rate between inlet and outlet was monitored in order to make sure it reached a stabilized value.

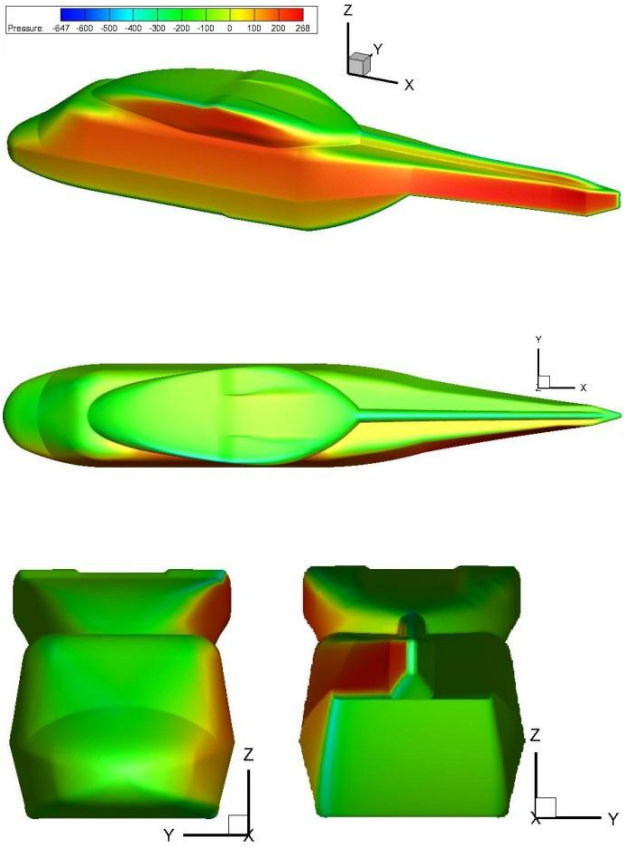

Figure 3: Contours of the Relative Total Pressure p_0 = 101325 [Pa].

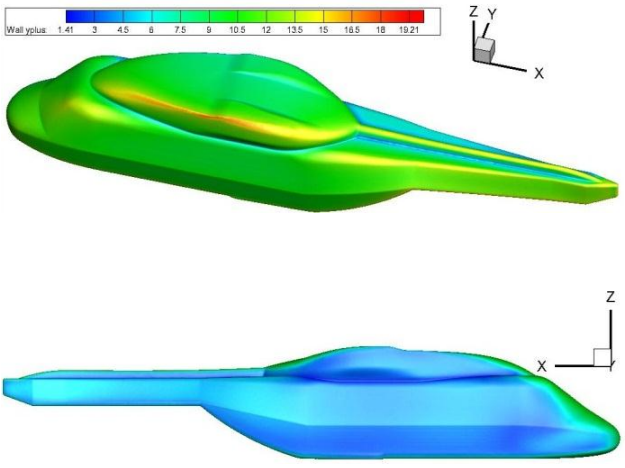

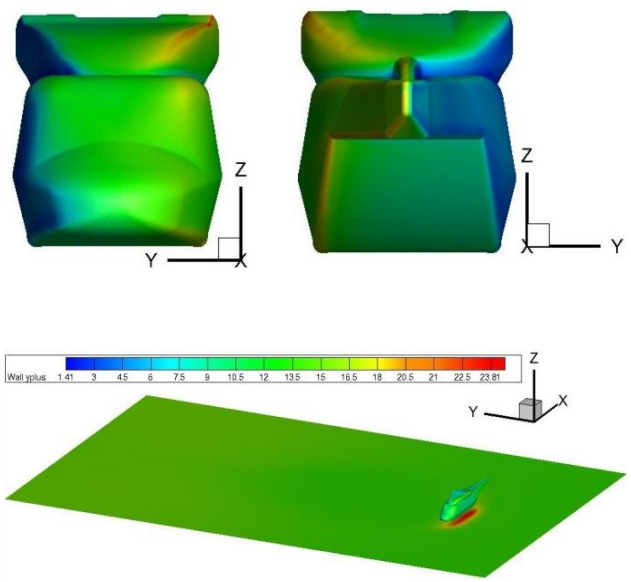

Figure 4: Contours of the Y+ coefficient.

In order to provide confidence on simulation results, an isolated fuselage configuration was first analysed and the associated simulation results compared against the available WT data. Then, the grounded fuselage was analysed providing the ground effect on the fuselage aerodynamic characteristics. In Table 3 a summary of the obtained results is reported.

	$\frac{F_D}{F_{D,EXP}}$	$\frac{F_L}{F_{L,EXP}}$	$\frac{M_X}{M_{X,EXP}}$	$\frac{M_Z}{M_{Z,EXP}}$
"ISOLATED" FUSELAGE CFD	0.91	1.14	0.98	0.90
"GROUND EFFECT" CFD	1.87	1.18	2.58	4.22

Table 3*:* Differences between CFD results and Experimental data

The comparison between CFD and experimental results shows that some differences are present in the normalized values. Nevertheless, the simulation could be considered valid despite the lateral wind which produce the extensively developed "turbulent field" downstream of the fuselage.

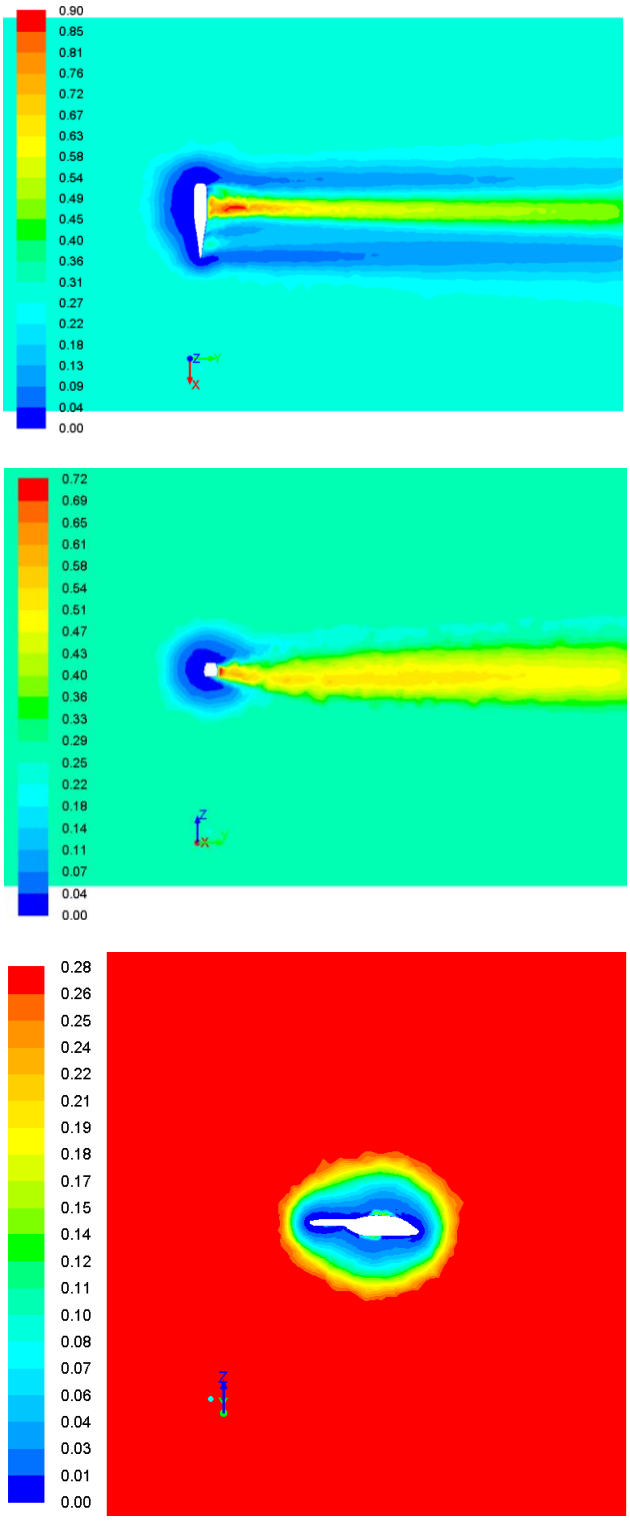

Figure 5 : Contours of the Turbulent Viscosity for "isolated" case

The drag force acting on the fuselage is doubled when the aircraft is nearby the ground, consequently both the pitch and yaw moments are increased with respect to the values encountered when considering a free stream flow over the fuselage.

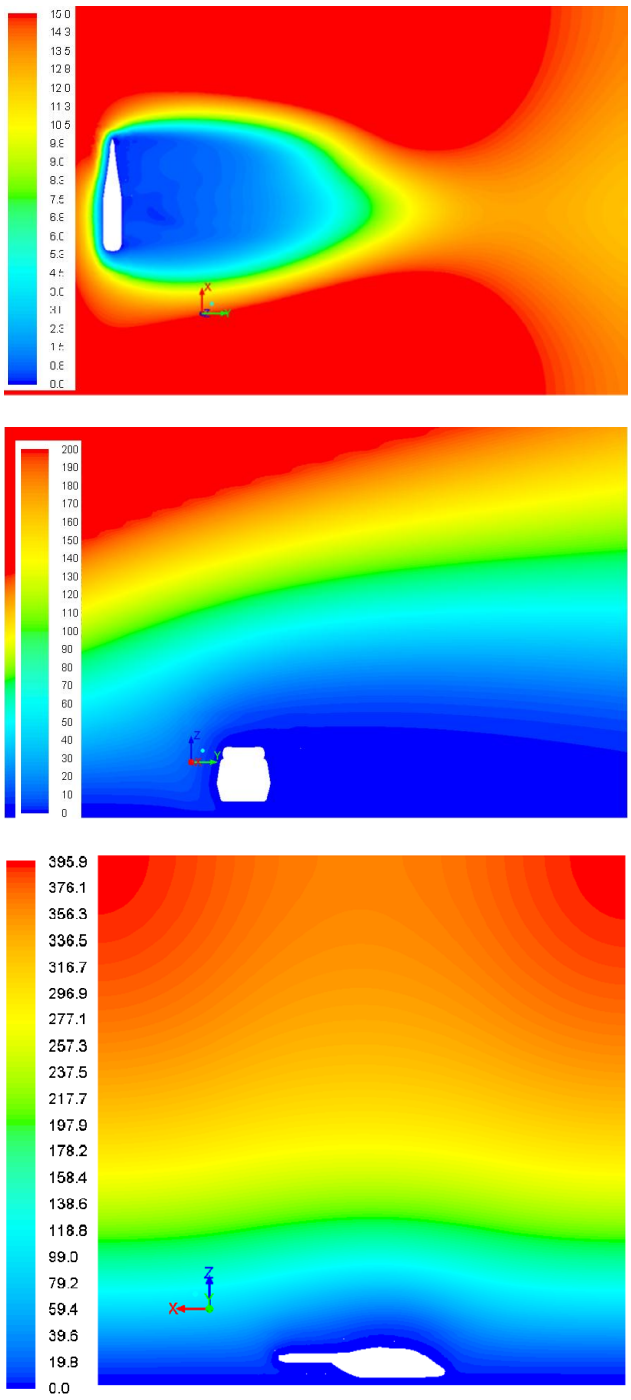

Figure 6 : Contours of the Turbulent Viscosity for "ground effect" case

The reduced model scale for the experiments will lead to an increase of the experiment complexity, caused by the scaled reduction of the vertically logarithmic distribution of mean wind speed and turbulence quantities due to related decrease in z_0 value. By the way the authors believe that it is necessary to put some efforts on it especially for the validation of the ground effect case.

5. Copyright Statement

6. References

[1] CRASTO G., PUDDU P., " *Numerical simulation of the ABL over complex terrain"* Ph.D. Thesis, University of Cagliari. (2007).

[2] BLOCKEN B., CARMELIET J., STATHOPOULOS T., *"CFD evaluation of wind speed conditions in passages between parallel buildings - effect of wall-function roughness modifications for the atmospheric boundary layer flow",* Journal of Wind Engineer and Industrial Aerodynamics 95 (2007) 941-962.

[3] BLOCKEN B., CARMELIET J., STATHOPOULOS T. *"CFD simulation of the atmospheric boundary layer: wall function problems",* Atmospheric Environment 41 (2007) 238-252.

[4] AA VV *"Modelling diabatic ABL using a RANS CFD code with a k-ε turbulence closure",* 13th Conference on Harmonization within Atmospheric Dispersion Modelling fot Regulatory Purposes (2010).

[5] P.J. RICHARDS, R.P. HOXEY *"Appropriate boundary conditions for computational wind engineering models using the k-ε turbulence model"* 1st International Symposium on Computational Wind Engineering (1992).

[6] W. ZDUNKOWSKI, A. BOTT "*Dynamics of the Atmosphere: A Course in Theoretical Meteorology"* Cambridge University Press (2003).

[7] D. A. SPERA *"Wind Turbine Technology"* Asme Press (1998).

[8] ANSYS Inc. "*Ansys Fluent 13.0 Documentation*" Ansys Inc. (2010).

[9] D.M. HARGREAVES, N.G. WRIGHT "*On the use of the k-ε model in commercial CFD software to model the neutral ABL"* Journal of Wind Engineer and Industrial Aerodynamics 95 (2007) 355-369.